Electronic Supplementary Information

Highly loaded fine PtCo intermetallic compounds on 3D N-doped porous graphene for enhanced sustained efficiency in PEMFCs

Zhihao Wang[a,b]†, Huihui Jin[c]†, Yizhou Hao[d], Cheng chen[a,e]*, Haifeng Lv[f]* and Daping He[a,c]*

[a]Sanya Science and Education Innovation Park of Wuhan University of Technology, Sanya 572000, China

[b]School of Materials Science and Engineering, Wuhan University of Technology, Wuhan 430070, China

[c]Hubei Engineering Research Center of RF-Microwave Technology and Application, School of Science, Wuhan University of Technology, Wuhan 430070, China

[d]Guangzhou Moxi Technology Co Ltd, Guangzhou 510535, China

[e]State Key Laboratory of Advanced Technology for Materials Synthesis and Processing, Wuhan University of Technology, Wuhan 430070, China

[f]PEM Fuel Cell Catalyst Research and Development Center, Shenzhen Academy of Aerospace Technology, Shenzhen 518057, China

**E-mail: chengchen@whut.edu.cn, lvhaifenganl@gmail.com, hedaping@whut.edu.cn*

† *These authors contributed equally to this work.*

Experimental Section

Material Characterization

Powder X-ray diffraction (P-XRD) measurements were performed on a Bruker D8 Advance X-ray diffractometer using Cu Kα radiation (λ = 1.5406 Å). Scanning electron microscope (SEM) was carried on a JSM-7100F. Transmission electron microscope (TEM) and high-resolution transmission electron microscope (HR-TEM) were collected on a JEM-2100F. Thermogravimetric analysis (TGA) was performed on a STA449F3 thermoanalyzer. Raman spectra were recorded on a Renishaw (INVIA) using Ar ion laser as excitation light source with a 514.5 nm excitation wavelength. X-ray photoelectron spectroscopy (XPS) analysis was carried on an ESCALAB 250Xi spectrometer using an Al-Kα radiation (1486 eV). Brunauer-Emmett-Teller (BET) specific surface areas were measured by N_2 physisorption on a Micromeritics ASAP 2020 system.

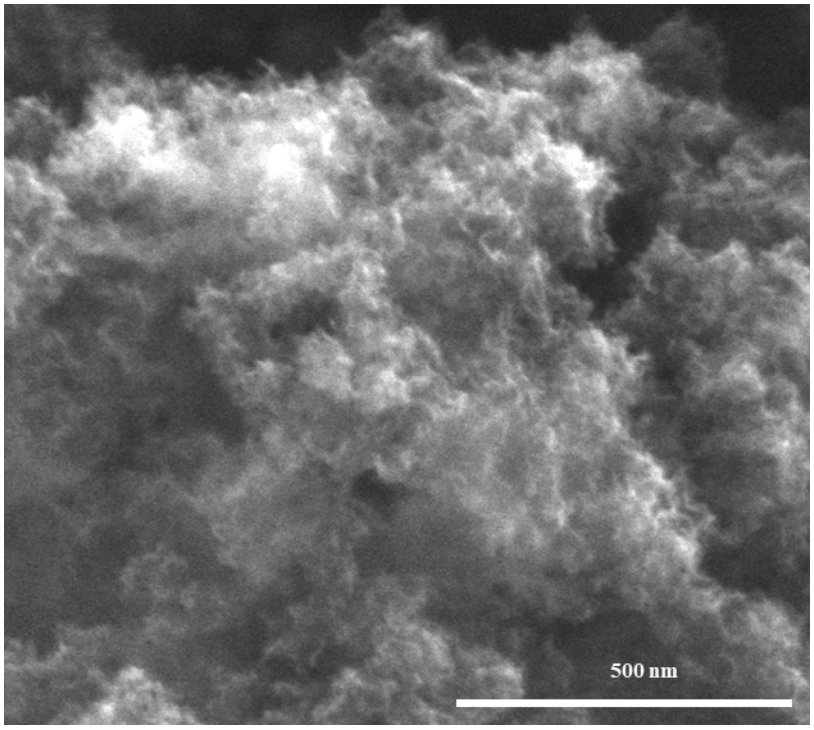

Figure S1 SEM image of HGG

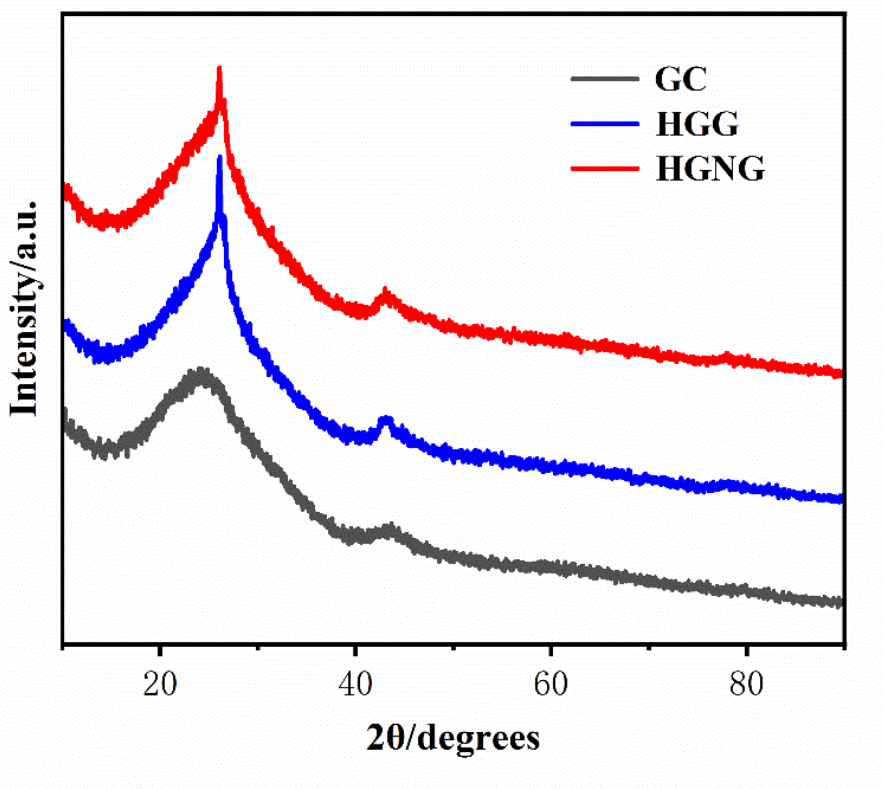

Figure S2 XRD patterns of GC, HGG and HGNG

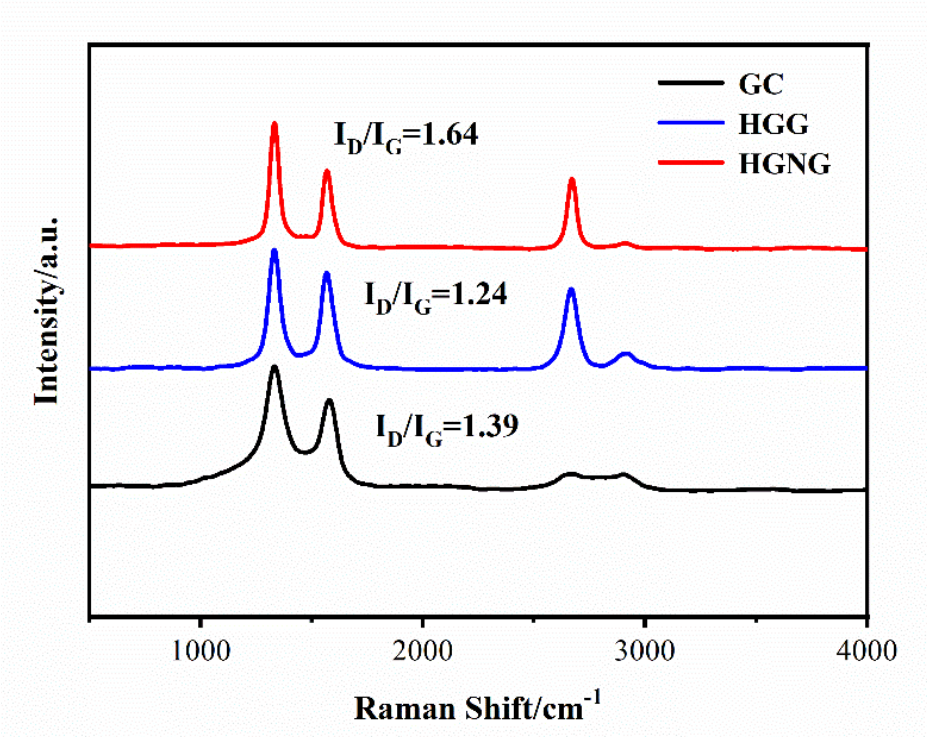

Figure S3 Raman spectra of GC, HGG, HGNG

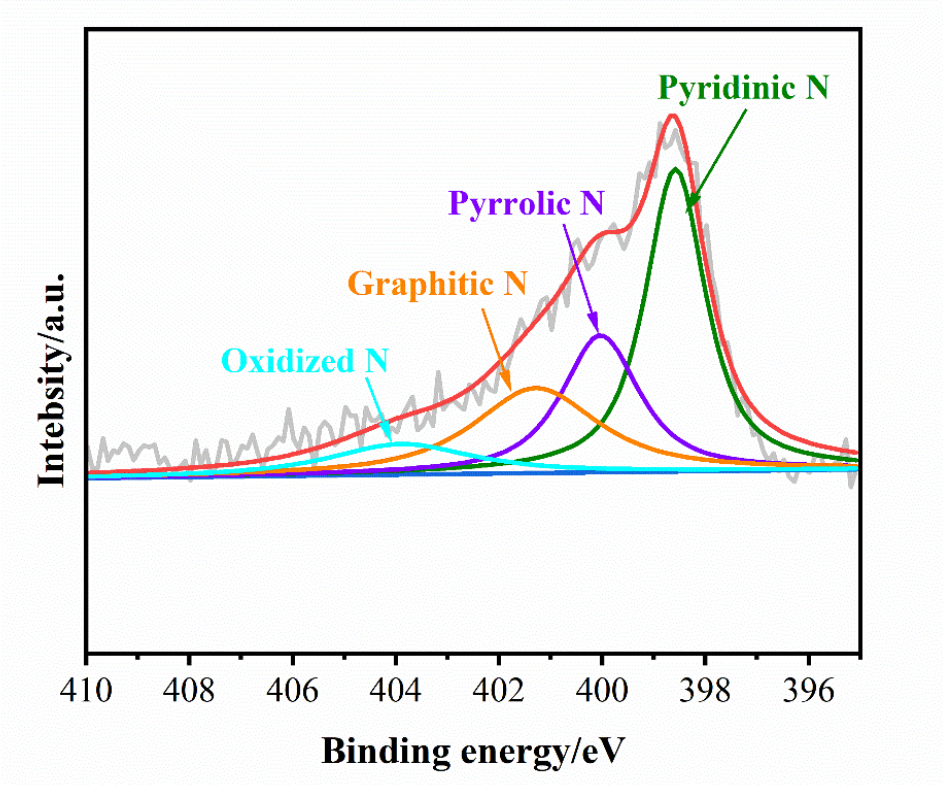

Figure S4 High resolution XPS spectrum of N 1s

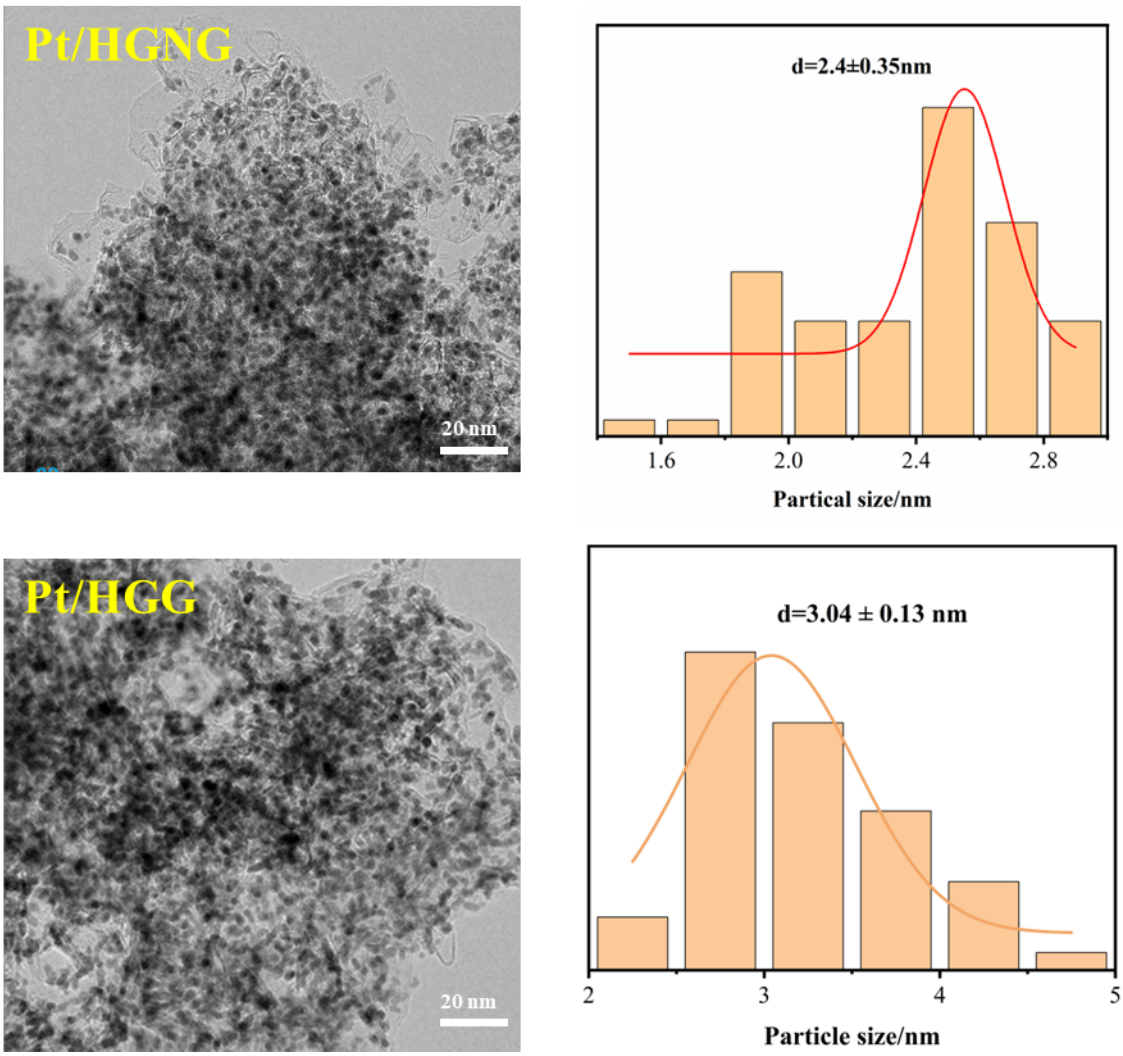

Figure S5 TEM images and corresponding particle distribution of Pt/HGNG and Pt/HGG.

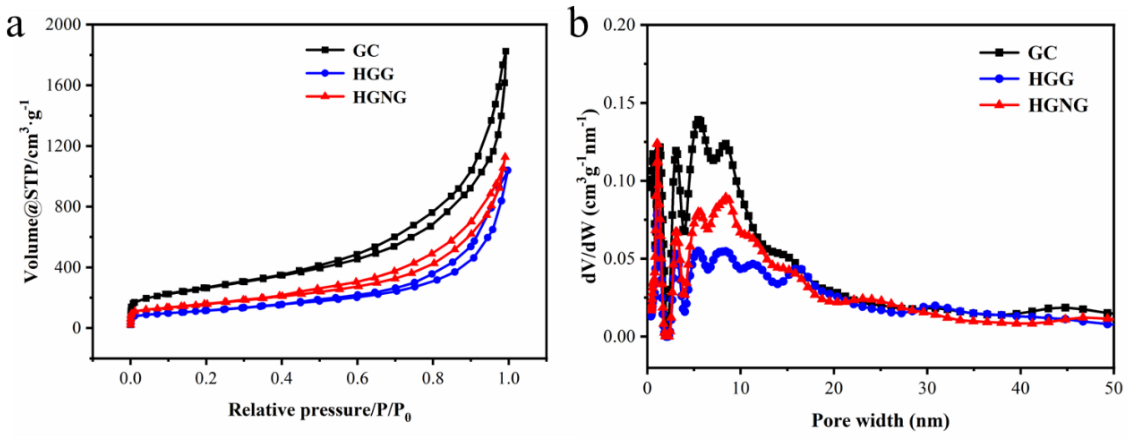

Figure S6 N_2 adsorption/desorption isotherms and pore size distribution of GC, HGG and HGNG

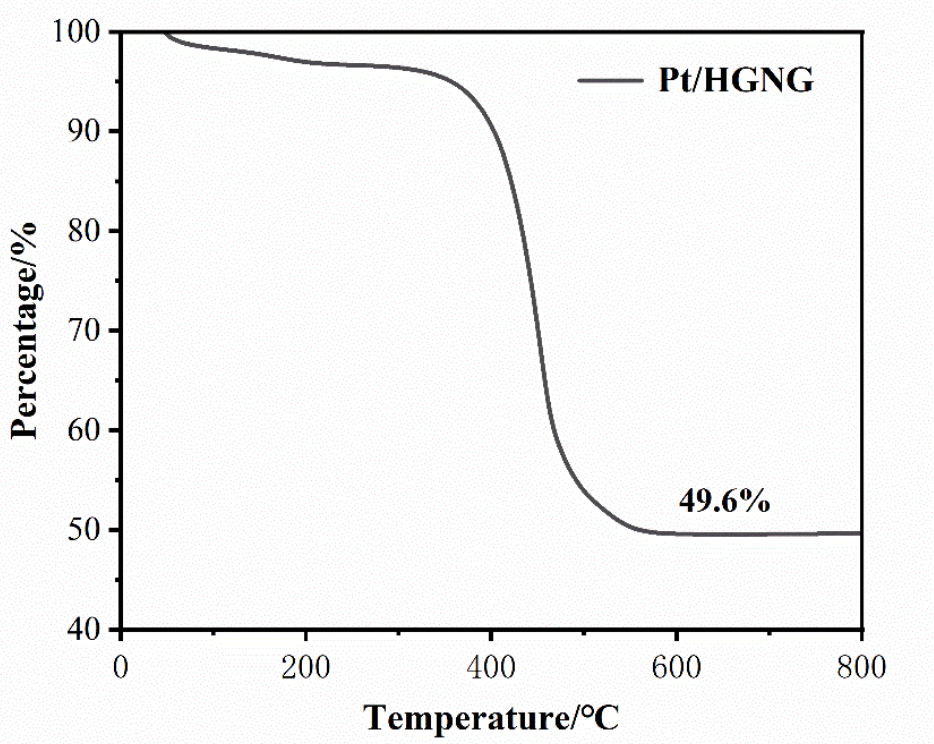

Figure S7 TG curve of Pt/HGNG under air atmosphere

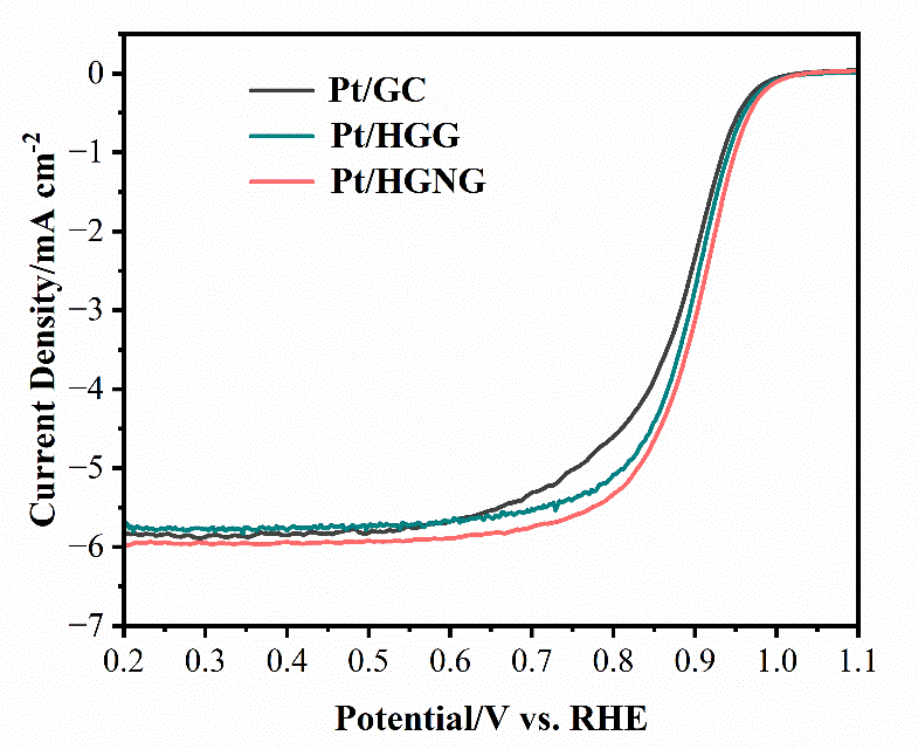

Figure S8 LSV curves of Pt/GC, Pt/HGG and Pt/HGNG.

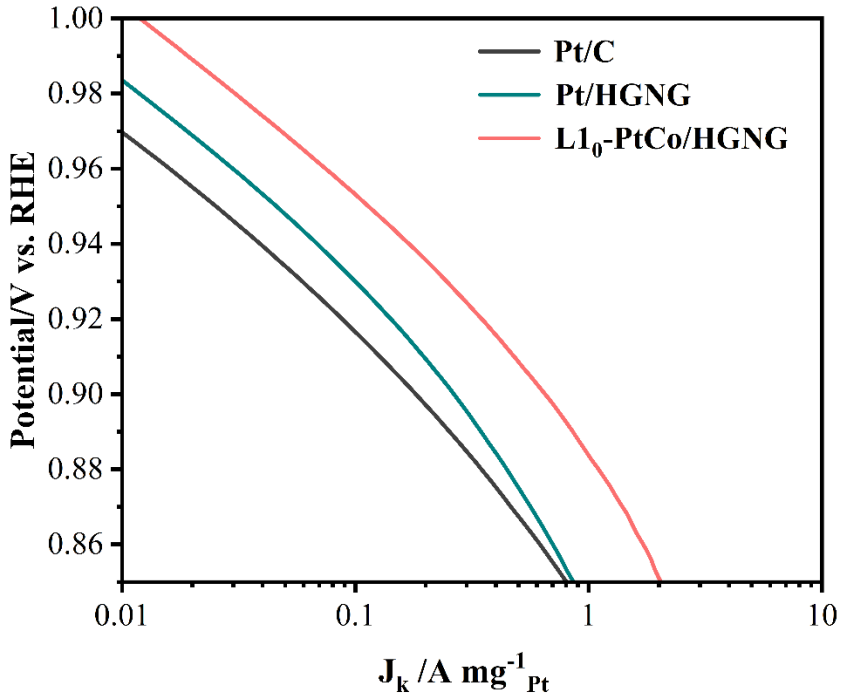

Figure S9 Mass activity Tafel plot of $L1_0$-PtCo/HGNG, Pt/HGNG and Pt/C

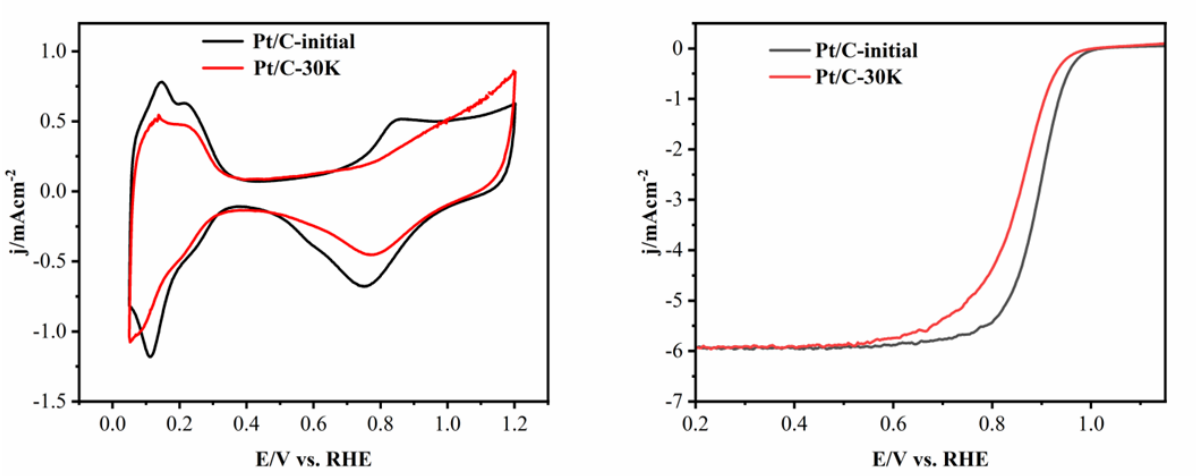

Figure S10 CV and LSV curves of Pt/C before and after 30K ADT cycles in 0.1M $HClO_4$ solution.

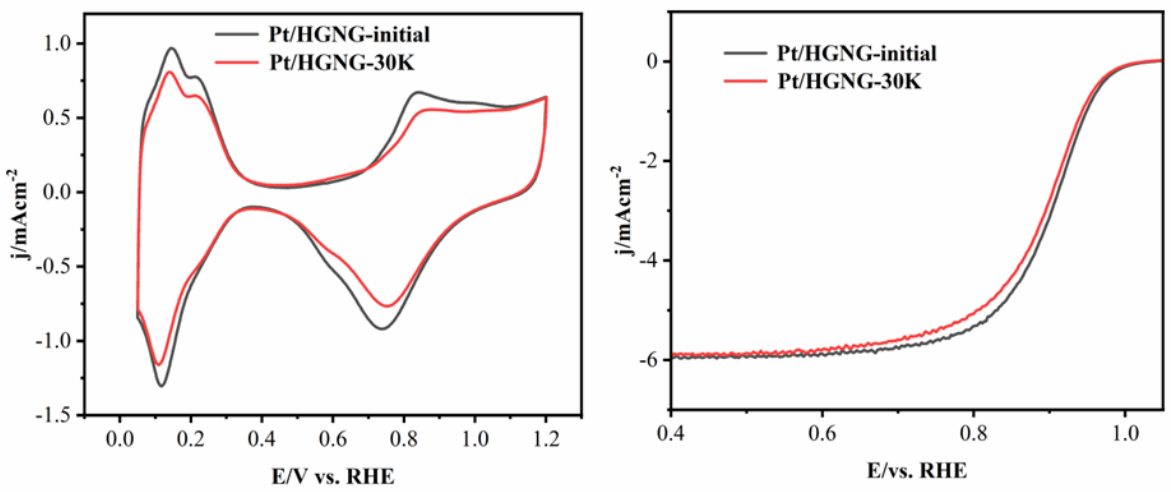

Figure S11 CV and LSV curves of Pt/HGNG before and after 30K ADT cycles in 0.1M $HClO_4$ solution.

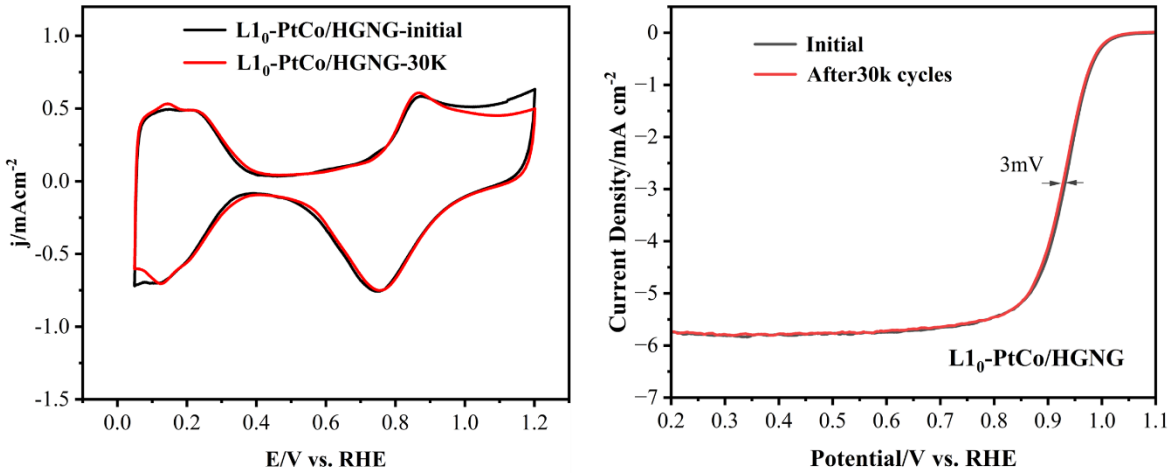

Figure S12 CV and LSV curves of $L1_0$-PtCo/HGNG before and after 30K ADT cycles in 0.1M $HClO_4$ solution.

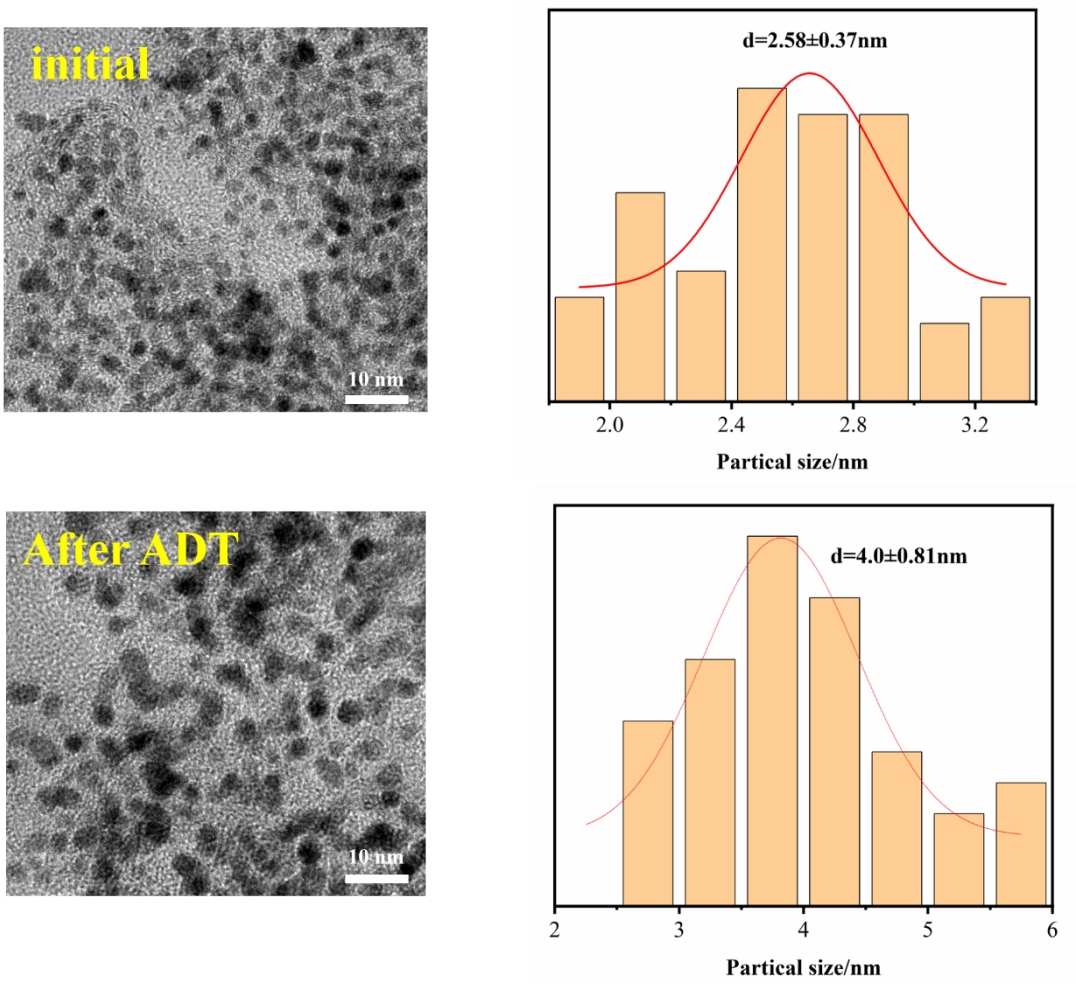

Figure S13 TEM images and corresponding size distribution of commercial Pt/C before and after ADT.

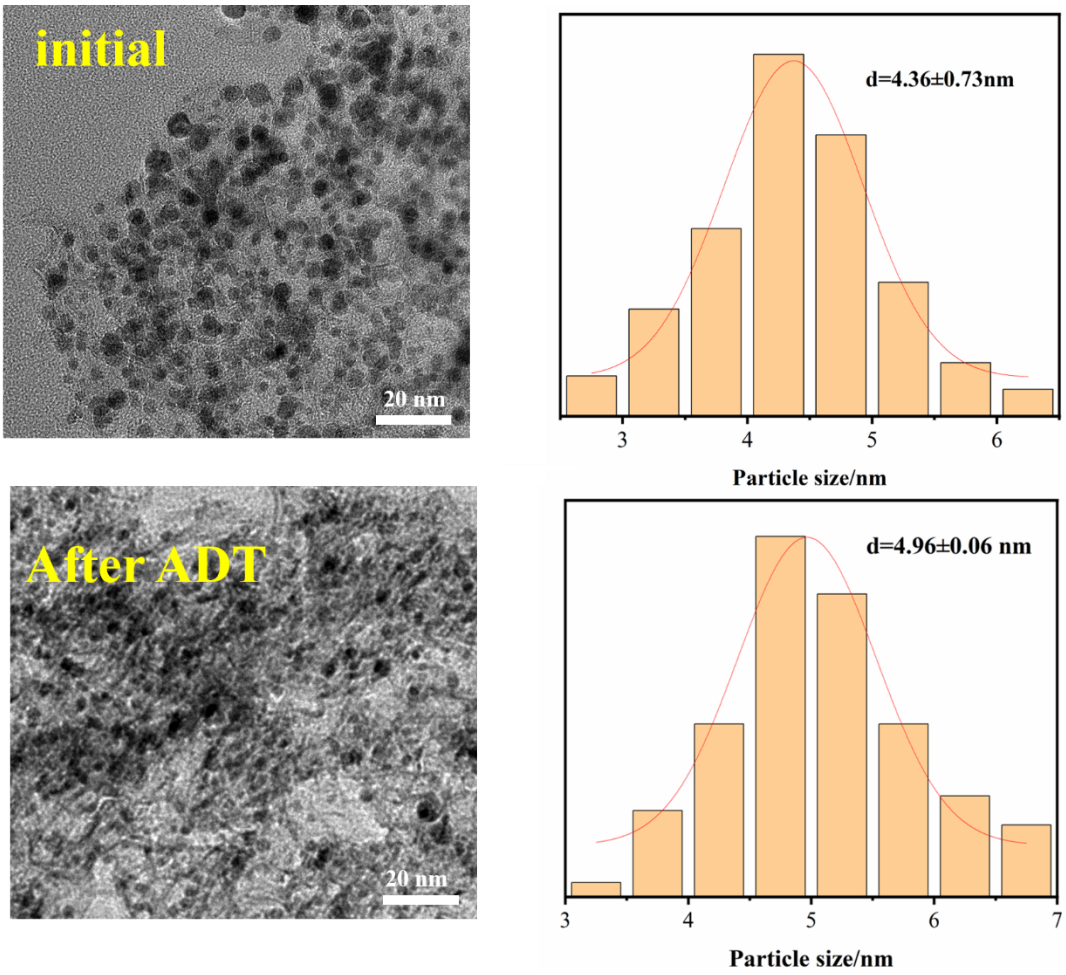

Figure S14 TEM images and corresponding size distribution of $L1_0$-PtCo/HGNG before and after ADT.

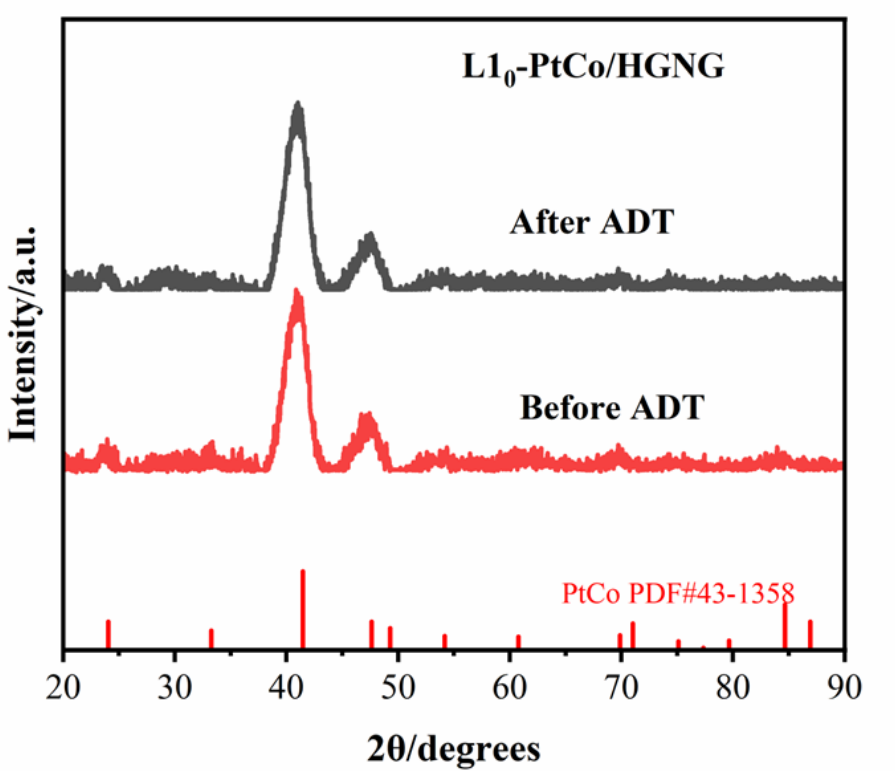

Figure S15 XRD patterns of $L1_0$-PtCo/HGNG before and after 30K ADT cycles.

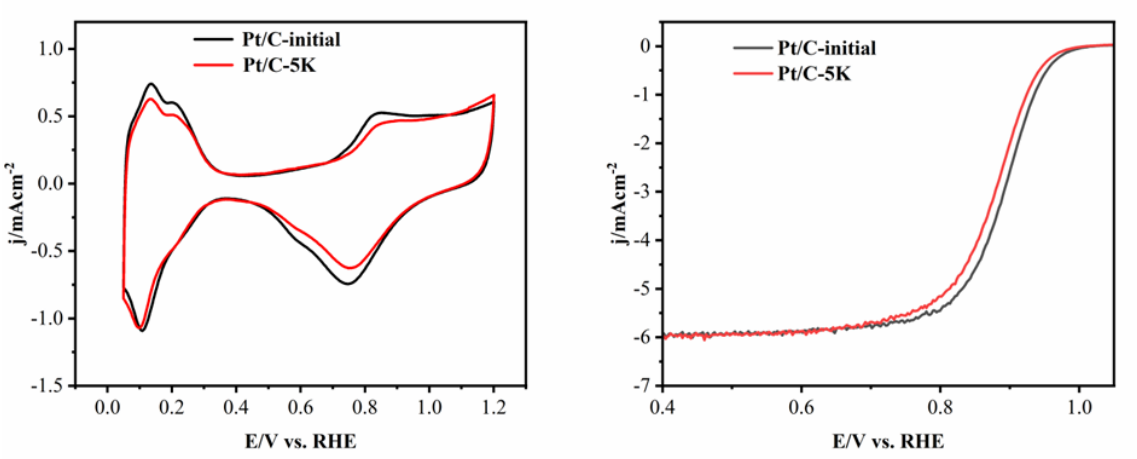

Figure S16 CV curve of Pt/C before and after 5K ADT cycles in 0.1M $HClO_4$ solution.

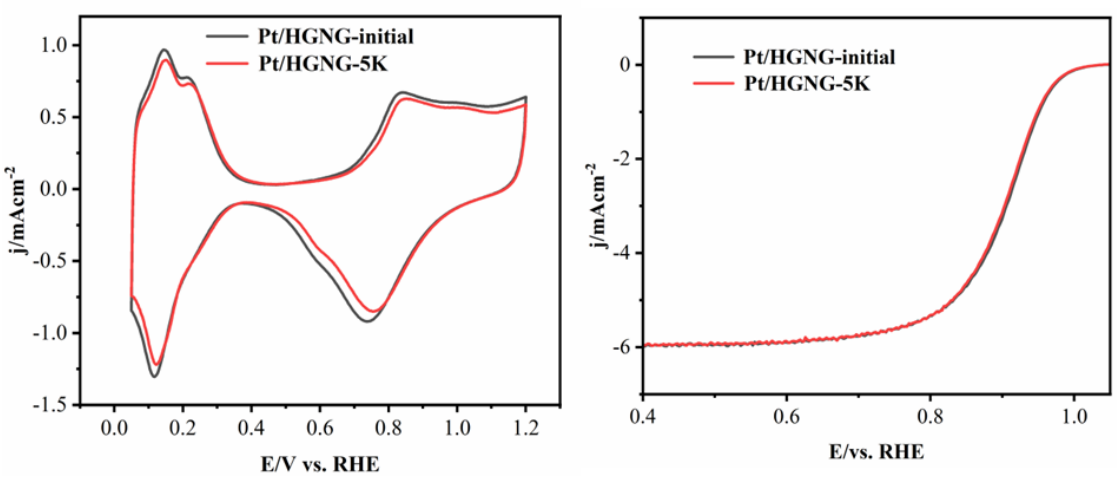

Figure S17 CV curve of Pt/HGNG before and after 5K ADT cycles in 0.1M $HClO_4$ solution.

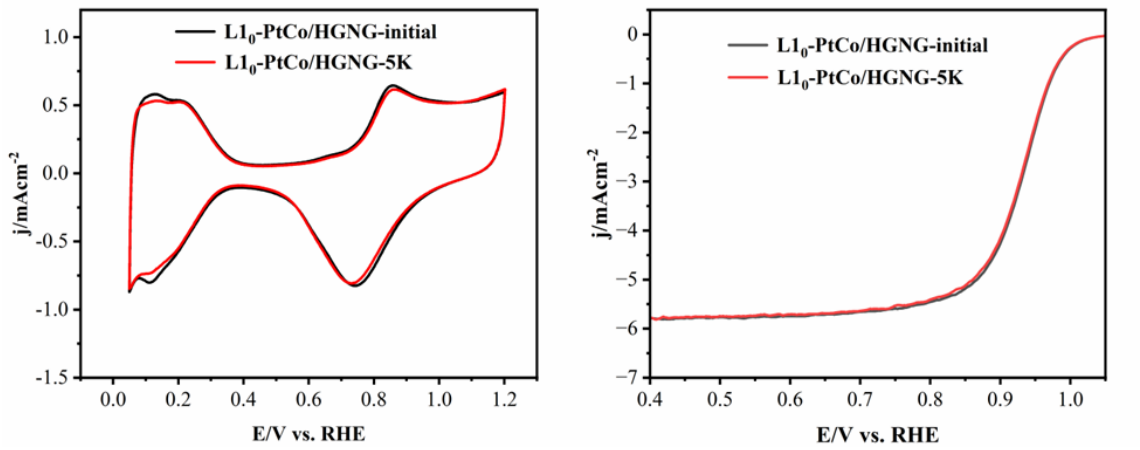

Figure S18 CV curve of $L1_0$-PtCo/HGNG before and after 5K ADT cycles in 0.1M $HClO_4$ solution.

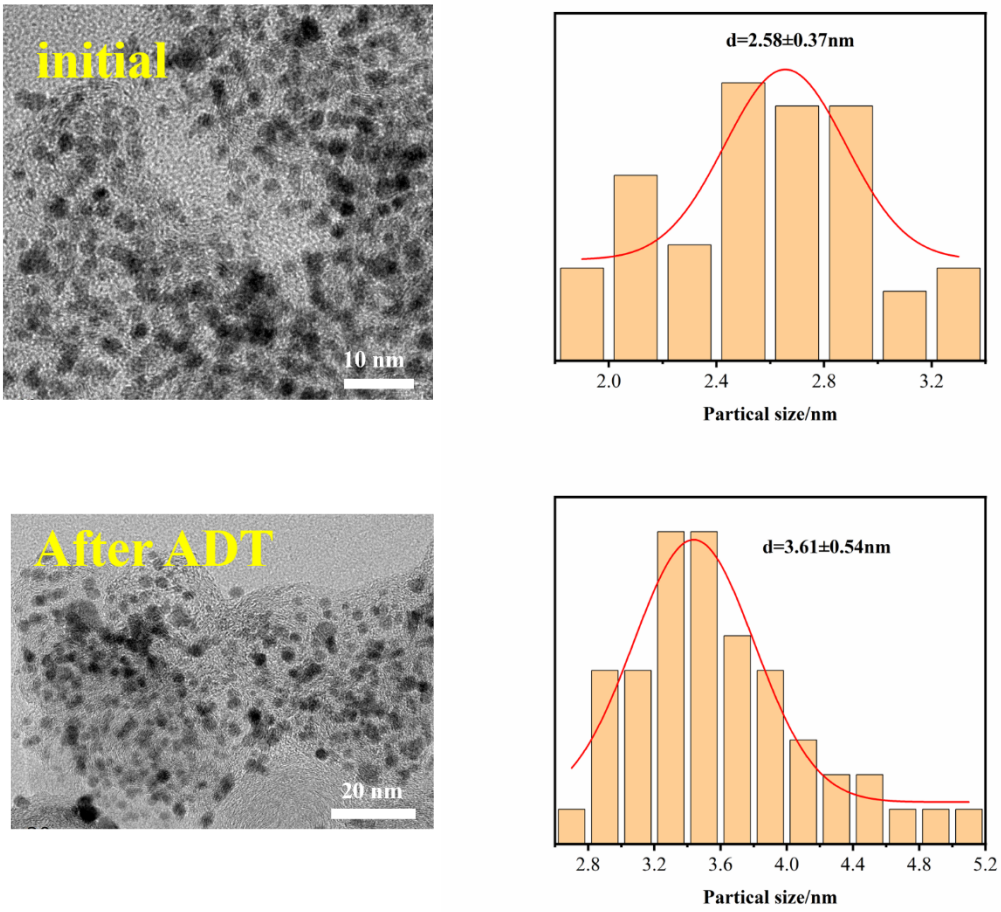

Figure S19 TEM images and corresponding size distribution of commercial Pt/C before and after ADT.

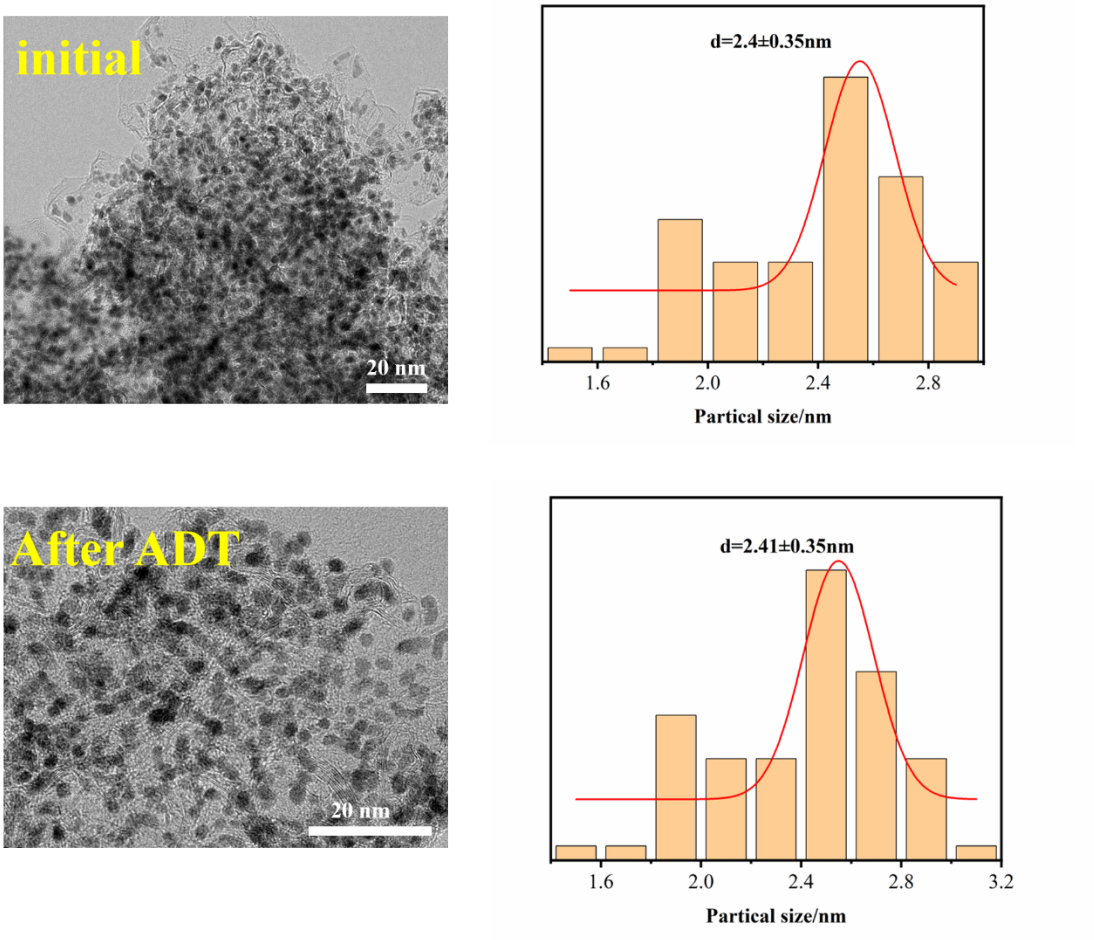

Figure S20 TEM images and corresponding size distribution of commercial Pt/HGNG before and after ADT.

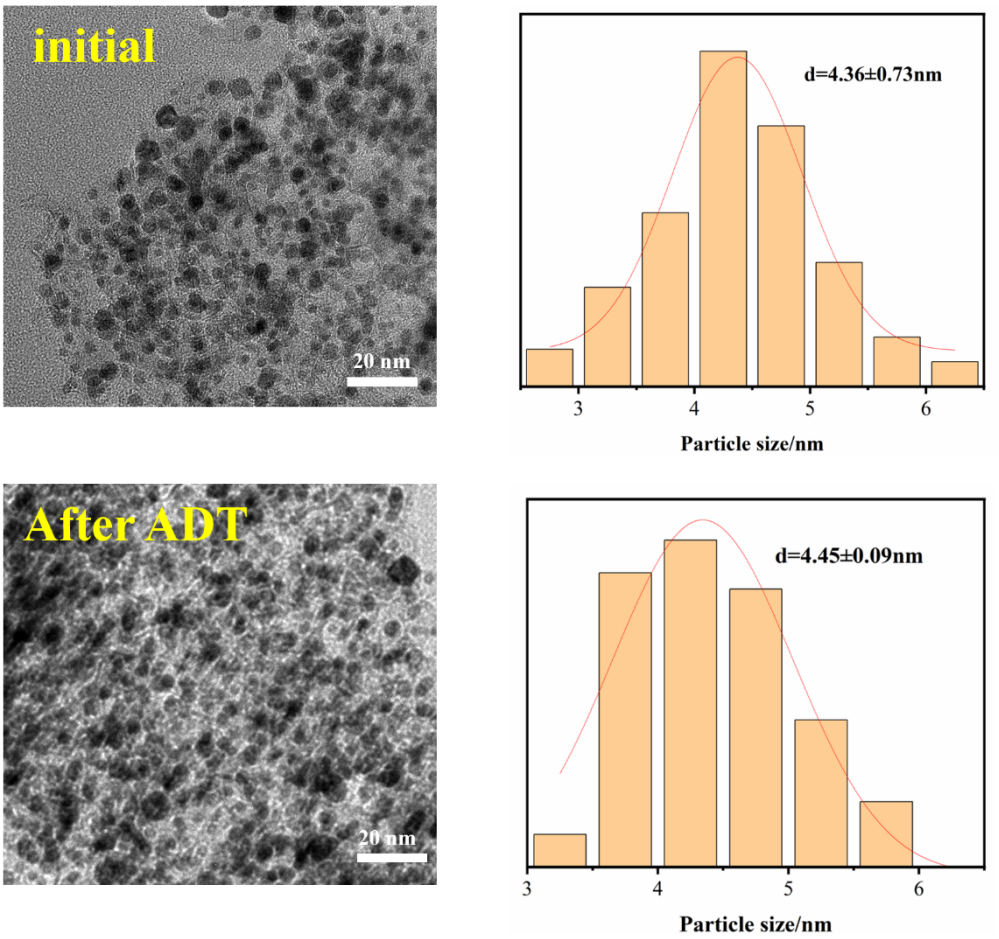

Figure S21 TEM images and corresponding size distribution of commercial $L1_0$-PtCo/HGNG before and after ADT.

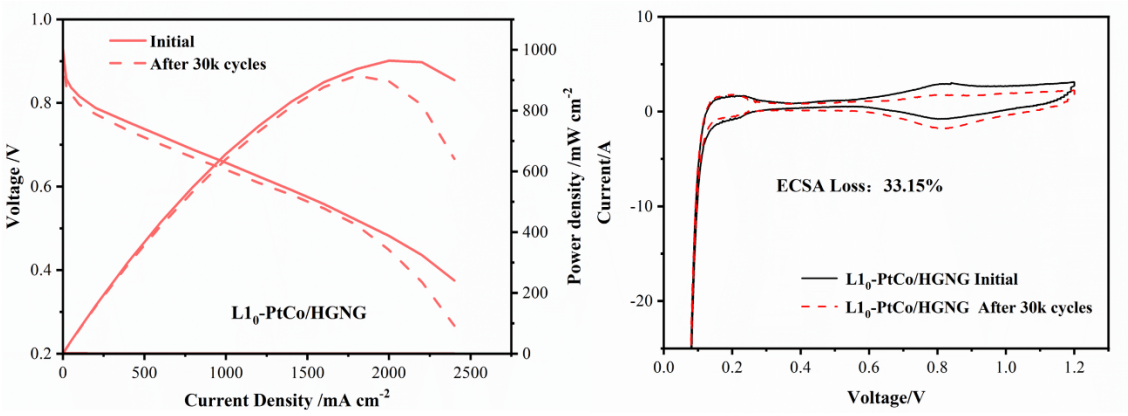

Figure S22 The polarization curves of H_2-air fuel cell with $L1_0$-PtCo/HGNG and CV curves before and after 30k cycles ADT.

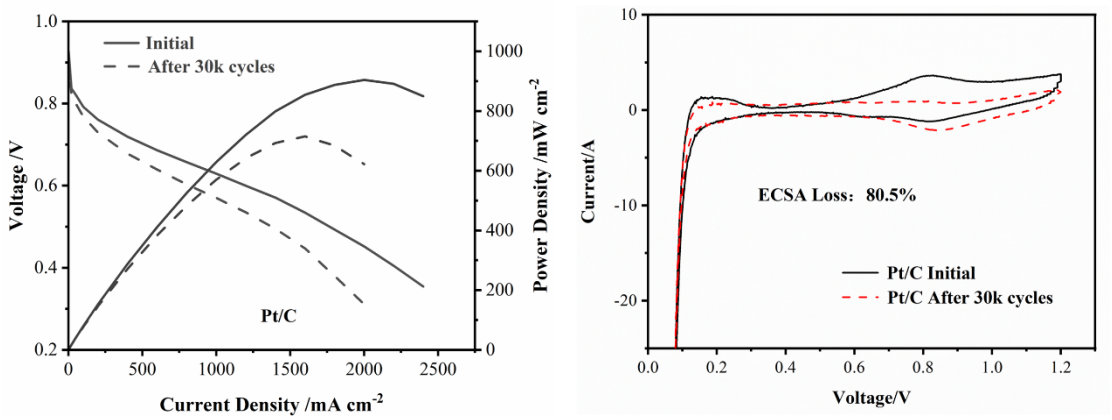

Figure S23 The polarization curves of H_2-air fuel cell with Pt/C and CV curves before and after 30k cycles ADT.

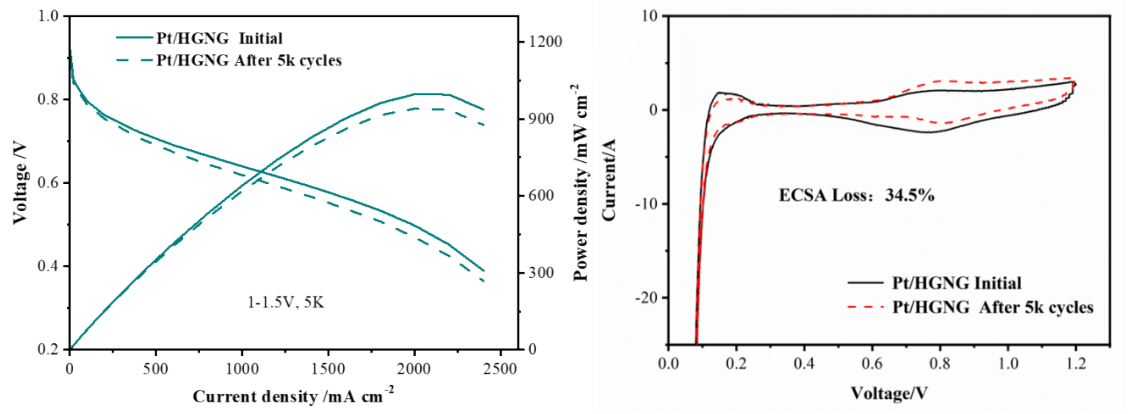

Figure S24 The polarization curves of H_2-air fuel cell with Pt/HGNG and CV curves before and after 5k cycles ADT.

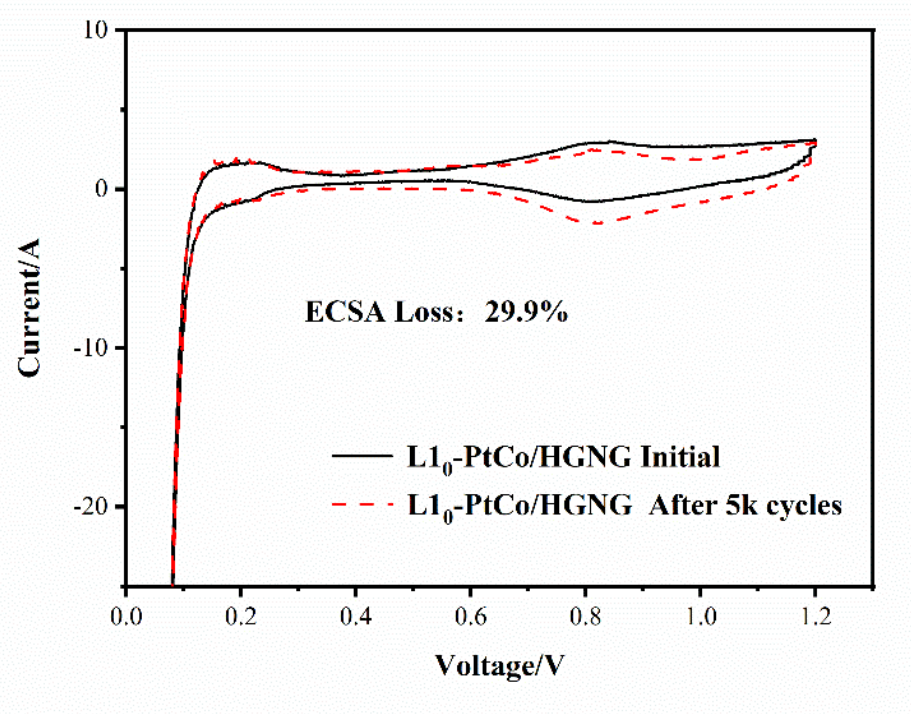

Figure S25 CV curves of $L1_0$-PtCo/HGNG before and after 5k cycles ADT.

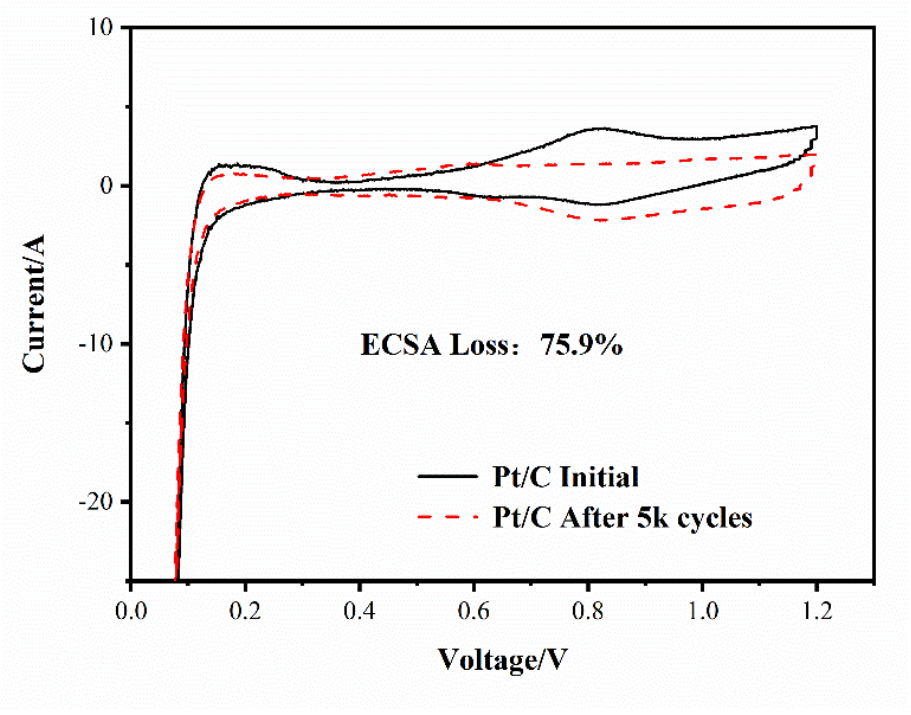

Figure S26 CV curves of commercial Pt/C before and after 5k cycles ADT.

Table S1 Contents of N, C, O element in HGG and HGNG obtained by XPS analysis.

	C (at)	N (at)	O (at)
HGG	97.9%	/	2.1%
HGNG	95.5%	2.58%	1.92%

Table S2 ICP results for Pt/HGNG and $L1_0$-PtCo/HGNG.

Catalysts	Pt (wt)	Co (wt)	Atom ratio (Pt:Co)
Pt/HGNG	49.8%	/	/
$L1_0$-PtCo/HGNG	45.9%	10.05%	58:42

Table S3 Comparison of H_2-Air fuel cell performance for recently reported Pt alloy electrocatalysts.

Catalysts	Cathode loading (mg_{Pt}/cm^2)	Peak power density (mW/cm^2)	Peak power density (W/mg_{Pt})	Pt loading (wt)	Refercences
$L1_0$-PtCo/HGNG	**0.1**	**964**	**9.64**	**45.9%**	**This work**
Commercial Pt/C	0.1	904	9.04	50%	This work
Pt1Co1-IMC@Pt/C	0.1	1130	11.3	44.7	S1
PCNMC-Co_8Zn_7	0.1	920	9.2	14.7%	S2
Pt_3Co/FeN_4-C	0.1	824	8.24	20%	S3
Pt/40Co-N-C-900	0.13	705	5.42	20%	S4
$L1_2$-Pt_3Co@ML-Pt/NPC_{10}	0.2	~1020	~5.1	22%	S5
Coplanar Pt/C NMs	0.1	553	5.5	20%	S6
IM-Pt_3Co	0.1	820	8.2	13.37%	S7
PtCo/KB-NH_2	0.1	960	9.6	24%	S8
$L1_0$-PtZn/Pt/C	0.104	750	7.2	20%	S9

References

S1. Q. Cheng. S. Yang, C. Fu, L. Zou, Z. Zou, Z. Jiang, J. Zhang and H. Yang, *Energy Environ. Sci.*, 2022, **15**, 278-286.

S2. Z. Chen, C. Hao, B. Yan, Q. Chen, H. Feng, X. Mao, J. Cen, Z. Tian, P. Tsiakaras and P. Shen, *Adv. Energy Mater.*, 2022, **12**, 2201600.

S3. Z. Qiao, C. Wang, C. Li, Y. Zeng, S. Hwang, B. Li, S. Karakalos, J. Park, A. Kropf, E. Wegener, Q. Gong, H. Xu, G. Wang, D. Myers, J. Xie, J. Spendelow and Gang Wu, *Energy Environ. Sci.*, 2021, **14**, 4948-4960.

S4. X. Wang, S. Hwang, Y. Pan, K. Chen, Y. He, S. Karakalos, H. Zhang, J. Spendelow, D. Su and G. Wu, *Nano Lett.*, 2018, **18**, 4163-4171.

S5. Z. Wang, S. Chen, W. Wu, R. Chen, Y. Zhu, H. Jiang, L. Yu and N. Cheng, *Adv. Mater.*, 2023, 35, 2301310.

S6. Y. Hu, M. Zhu, X. Luo, G. Wu, T. Chao, Y. Qu, F. Zhou, R. Sun, X. Han, H. Li, B. Jiang, Y. Wu and X. Hong, *Angew. Chem. Int. Ed.*, 2021, **60**, 6533.

S7. M. Zhu, H. Zhang, Y. Hu, F. Zhou, X. Gao, D. He, X. Zhao, C. Zhao, J. Wang, W. Tie, X. Tian, B. Wang, T. Yao, H. Zhou, Z. Wang, J. Wang, W. Guo and Y. Wu, *ACS Catal.*, 2024, **14**, 5858-5867.

S8. Q. Gong, H. Zhang, H. Yu, S, Jeon, Y. Ren, Z. Yang, C. Sun, E. Stach, A. Fouche, Y. Yu, M. Smart, G. Filippelli, D. Cullen, P. Liu and J. Xie, *Matter*, 2023, **6**, 963-982.

S9. J. Liang, Z. Zhao, N. Li, X. Wang, S. Li, X. Liu, T. Wang, G. Lu, D. Wang, B.-J. Hwang, Y. Huang, D. Su and Q. Li, *Adv. Energy Mater.*, 2020, **10**, 2000179.